ACS APPLIED MATERIALS & INTERFACES

Research Article

www.acsami.org

Surface Modification by Allylamine Plasma Polymerization Promotes Osteogenic Differentiation of Human Adipose-Derived Stem Cells

Xujie Liu,[†] Qingling Feng,*[,†,‡] Akash Bachhuka,[§] and Krasimir Vasilev[§,∥]

[†]State Key Laboratory of New Ceramics and Fine Processing, School of Materials Science and Engineering, Tsinghua University, Beijing 100084, China

[‡]Key Laboratory of Advanced Materials of Ministry of Education of China, School of Materials Science and Engineering, Tsinghua University, Beijing 100084, China

[§]Mawson Institute, University of South Australia, Mawson Lakes 5095, Australia

[∥]School of Advanced Manufacturing, University of South Australia, Mawson Lakes 5095, Australia

Supporting Information

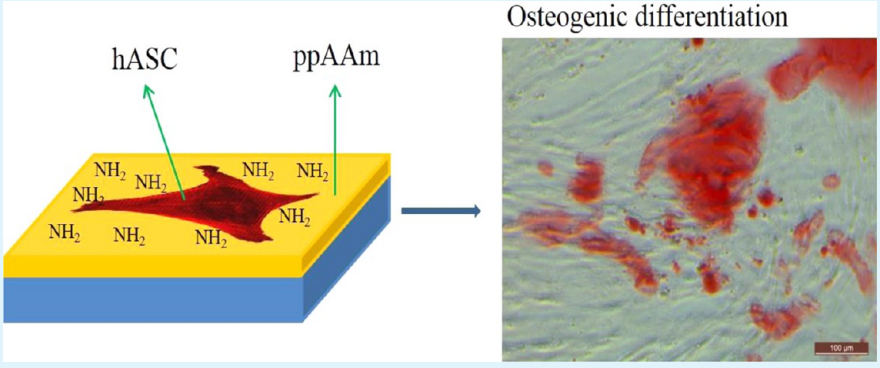

ABSTRACT: Tuning the material properties in order to control the cellular behavior is an important issue in tissue engineering. It is now well-established that the surface chemistry can affect cell adhesion, proliferation, and differentiation. In this study, plasma polymerization, which is an appealing method for surface modification, was employed to generate surfaces with different chemical compositions. Allylamine (AAm), acrylic acid (AAc), 1,7-octadiene (OD), and ethanol (ET) were used as precursors for plasma polymerization in order to generate thin films rich in amine ($-NH_2$), carboxyl ($-COOH$), methyl ($-CH_3$), and hydroxyl ($-OH$) functional groups, respectively. The surface chemistry was characterized by X-ray photoelectron spectroscopy (XPS), the wettability was determined by measuring the water contact angles (WCA) and the surface topography was imaged by atomic force microscopy (AFM). The effects of surface chemical compositions on the behavior of human adipose-derive stem cells (hASCs) were evaluated *in vitro*: Cell Count Kit-8 (CCK-8) analysis for cell proliferation, F-actin staining for cell morphology, alkaline phosphatase (ALP) activity analysis, and Alizarin Red S staining for osteogenic differentiation. The results show that AAm-based plasma-polymerized coatings can promote the attachment, spreading, and, in turn, proliferation of hASCs, as well as promote the osteogenic differentiation of hASCs, suggesting that plasma polymerization is an appealing method for the surface modification of scaffolds used in bone tissue engineering.

KEYWORDS: *plasma polymerization, surface modification, osteogenic differentiation, human adipose-derived stem cell, bone tissue engineering*

1. INTRODUCTION

Bone tissue engineering has emerged as a promising route for the treatment of healing bone defects.[1] Tissue engineering aims to fabricate biologically inspired scaffolds capable of integrating with native tissue and/or stimulate the body's innate repair mechanisms to regenerate damaged tissue and restore function.[2] Within the tissue-engineering paradigm, cells, scaffolds, and biological molecules are generally referred to the key components.[3] Thus, it is vital to understand the relationship between the cells and the materials used in bone tissue engineering. It has been demonstrated that the topography,[4,5] chemical compositions,[6] mechanical properties,[7] and architecture[8] of scaffolds are able to interact and influence cell behavior, including the attachment, proliferation, migration, and differentiation.

In bone tissue engineering, the supplement of autologous osteocytes is limited.[9] Consequently, increasing attention has focused upon the use of stem cells, such as bone marrow

Received: April 9, 2014
Accepted: June 3, 2014
Published: June 3, 2014

mesenchymal stem cells (BM-MSCs) and adipose-derived stem cells (ASCs). Similar to BM-MSCs, ASCs have the potential to differentiate into osteocytes, chondrocytes, myocytes, and adipocytes, etc. Moreover, ASCs are easier to largely isolate from adipose tissue using liposuction, which does not require painful procedures or cause donor site injury.[10] Therefore, research has substantially progressed on the use of ASCs, instead of osteoblasts or BM-MSCs, as cell source for bone tissue engineering.[11]

When using ASCs in bone tissue engineering, it is important to understand how the scaffold influences the osteogenic differentiation of ASCs. Besides the bulk properties of scaffolds (biodegradability, strength, etc.), the surface of a material also plays a key role in controlling the stem cell fate as the cells will attach to the surface and, in turn, respond differently to the different surface properties. It has been demonstrated that the surface chemistry can affect protein adsorption and the binding of different integrins, in this way, affect the cell behavior.[12−14] To evaluate surface chemistry-induced cellular responses, several methods have been employed, such as silane-modification[15,16] and alkanethiol self-assembled monolayers (SAMs).[17] These two methods have been employed to study the adhesion, proliferation, and osteogenic differentiation of BM-MSCs[18] and ASCs.[19] Although the two methods are both excellent as model systems,[20] they are limited to the modification of a specific substrate material and not suitable for application on scaffolds used in bone tissue engineering. Silane modification is a technique to introduce different functional groups on glass or silica substrates. When SAMs of alkanethiol are used, a metal substrate (i.e., Au) is usually required. Alternately, plasma polymerization has emerged as a utility for fabrication of stable, easy to sterilize (i.e., irradiation), pinhole-free polymeric coatings with high retention of functional groups onto a wide range of substrate materials at a low cost.[21,22] Furthermore, these coatings can be easily engineered to suit a particular purpose.[23] All these benefits and, particularly, the capacity to apply functional coatings on any type of substrate materials make plasma polymerization an attractive technique for biomedical applications. When introducing plasma polymerization in bone tissue engineering, it is important to choose a certain precursor which can generate a certain surface chemical state to promote osteogenesis.

The goal of this study is to explore the capacity of functional plasma-polymerized coatings to promote osteogenesis of ASCs. Allylamine (AAm), acrylic acid (AAc), 1,7-octadiene (OD), and ethanol (ET) were selected as precursors for plasma polymerization in order to generate coatings rich in amine ($-NH_2$), carboxyl (−COOH), methyl ($-CH_3$), and hydroxyl (−OH) chemical groups, respectively. These functionalities were selected because they naturally exist within biological systems.[13] The behavior of human ASCs (hASCs), especially the osteognic differentiation on such modified substrates was investigated *in vitro*. These results are meaningful for the application of plasma polymerization in the surface modification of scaffolds used in bone tissue engineering.

2. MATERIALS AND METHODS

2.1. Surface Modification by Plasma Polymerization. Plasma polymerization was carried out in a custom-built parallel plate reactor previously described.[24,25] Allylamine (AAm), acrylic acid (AAc), 1,7-octadiene (OD), and ethanol (ET) were used as precursors for plasma deposition in order to generate thin films rich in amine ($-NH_2$), carboxyl (−COOH), methyl ($-CH_3$), and hydroxyl (−OH) chemical groups, respectively. Clean coverslips (diameter: 13 mm) were used as substrates. The chamber was evacuated to pressure of 1×10^{-3} mbar before deposition. The deposition condition was described in Table 1. The following abbreviations: ppAAm, ppAAc, ppOD and ppET were used throughout the text to denote plasma polymerized films deposited from vapor of allylamine, acrylic acid, 1,7-octadiene, and ethanol, respectively.

Table 1. Deposition Condition of Plasma Polymerization

	precursor	pressure (mbar)	power (W)	time (s)
ppAAm	allylamine	2.1×10^{-1}	40	120
ppAAc	acrylic acid	2.1×10^{-2}	10	120
ppOD	1,7-octadiene	2.1×10^{-2}	20	120
ppET	ethanol	1×10^{-1}	10	600

2.2. Surface Characterization. The samples should be sterilized when used in cell culture or tissue engineering. ^{60}Co irradiation was employed as sterilization method. To take this into account, all surface analysis were performed after ^{60}Co irradiation.

2.2.1. X-ray Photoelectron Spectroscopy. X-ray photoelectron spectroscopy (XPS) was carried on a photoelectron spectrometer (Model ESCALAB-250Xi) equipped with a monochromatic Al Kα X-ray source. The survey scans were performed on each sample at pass energies of 100 eV and step of 1 eV to identify and quantify the elements present. The C 1s high-resolution spectra were also recorded using pass energy of 20 eV and step of 0.05 eV. All binding energies were calibrated with reference to the aliphatic carbon at C 1s = 284.8 eV. The C 1s spectra were fitted using XPSPEAK 4.1 software. The best fitting was performed with a full width at half maximum (fwhm) value of 1.50 ± 0.10 eV for all components.

2.2.2. Water Contact Angle Measurement. Water contact angles were measured by the sessile drop method on a contact angle meter (Model JC2000C1, Powereach, China). A 4-μL droplet of pure water was carefully added on the surfaces of different samples. Images of the drops were captured immediately with an adjacent camera. The contact angle was analyzed using the JC2000 software. The measurements were taken at four different places for one sample.

2.2.3. Atomic Force Microscopy. Atomic force microscopy (AFM) studies were carried out with an atomic force microscopy (AFM) microscope (Model SPM-9600, Shimadzu, Japan) to observe the topography of the samples. Samples were imaged in a tapping mode with an area of 1 μm × 1 μm.

2.3. Cell Culture. Human adipose-derived stem cells (hACSs) were expanded in low-glucose Dulbecco's modified Eagle's medium (LG-DMEM, Invitrogen, USA), containing 10% fetal bovine serum (FBS, Invitrogen, USA), 100 μg/mL streptomycin, and 100 U/mL penicillin (growth medium, GM) and used as passage 4. The ability of osteogenesis and adipogenesis was evaluated *in vitro* before use. The sterilized samples by ^{60}Co irradiation were placed in 24-well plates (Corning, USA). hASCs were seeded on the samples at a density of 10 000 cells/well and allowed to adhere for 24 h under standard culture conditions (5% CO_2, 37 °C). The supernatants were replaced with fresh medium every 2 or 3 days.

2.3.1. Cytoskeleton Staining for Morphology. The cells were cultured in GM for 24 h. The cells attached on the samples were washed with 0.01 M PBS (Corning, USA) twice,

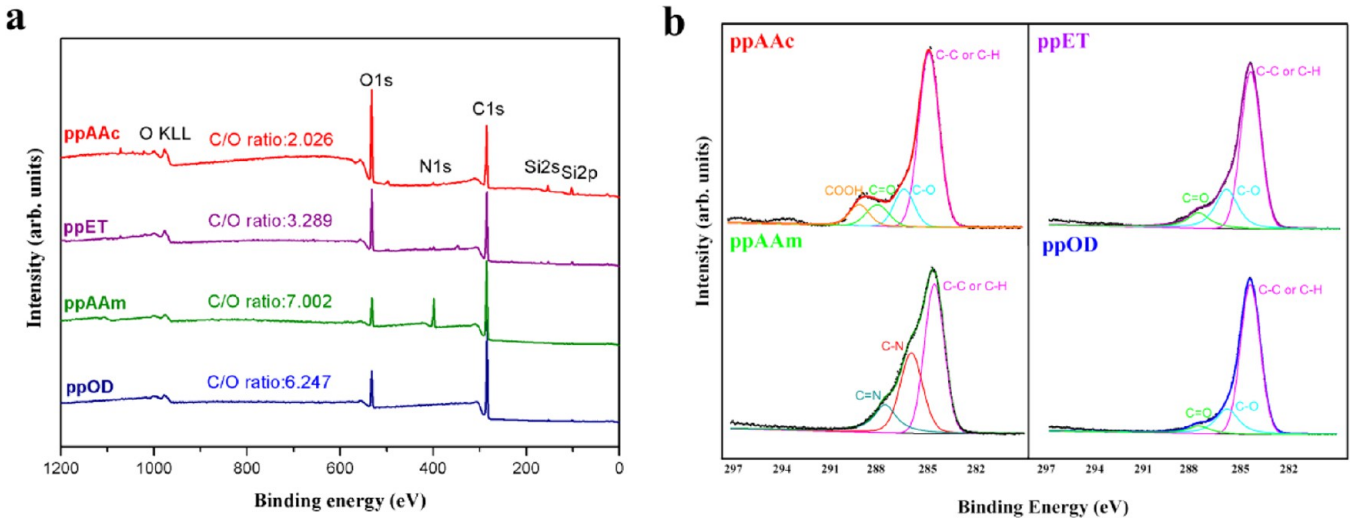

Figure 1. XPS spectra of different samples: (a) survey spectra and (b) high resolution of C 1s spectra.

fixed with 4% (w/v) paraformaldehyde (in PBS) for 30 min, and permeabilized with 0.1% Triton X-100 (in PBS) for 10 min. Thereafter, the cells were stained for the cytoskeletal filamentous actin and nuclei with 5 μg/mL phalloidin-TRITC (Sigma, USA) for 40 min at room temperature and 2 μg/mL of 4′,6-diamidino-2-phenylindole (DAPI) for 30 min at 37 °C, respectively. The samples were imaged under a fluorescence microscope (Leica, Germany).

2.3.2. CCK-8 Assay for Proliferation. A Cell Count Kit-8 (CCK-8, Dojindo, Japan) was used to quantitatively evaluate the cell proliferation. The cells were cultured in GM with (+) and without (−) osteogenic supplement (OS, 10^{-7} M dexamethasone, 10 mM β-glycerophosphate disodium, 50 μg/mL ascorbic acid) for 2 and 8 days. Then, CCK-8 with a 10% vol of the medium was added into the wells and incubated for 3 h at 37 °C. CCK-8 can be transformed to orange-colored formazan in the presence of dehydrogenases in living cells. One hundred microliters (100 μL) of the reaction solution was transferred into a new 96-well plate and the absorbance (OD) of the solution was measured by a microplate reader (Biorad, USA) at 450 nm. The experiments were carried out in sextuplicate.

2.3.3. Alkaline Phosphatase (ALP) Activity Assay. The cells were cultured in GM with (+) and without (−) OS for 10 days. The cells then were washed with precooled PBS for three times and lysed using RIPA lysis buffer (Beyotime, China) containing 1 mM phenylmethanesulfonyl fluoride (PMSF) for 15 min on ice. Each lysate was collected and centrifuged at 12 000 rpm for 10 min at 4∘C. The supernatants were analyzed using an ALP testing kit (Jiancheng, China) according to the guidelines set by their manufacturer. The ALP activity was normalized by the total protein content determined with the BCA Assay Kit (Beyotime, China), according to the company's guidelines. The experiments were carried out in quadruplicate.

2.3.4. Alizarin Red S Staining. The cells were cultured in GM with (+) OS for 14 days. The cells were washed with PBS (0.01 M) twice, fixed with 4% paraformaldehyde for 30 min, then stained with 1% Alizarin Red S (pH at 4.2) for 15 min at 37 °C. The samples were imaged under a phase-contrast microscope (Leica, Germany). To quantify the retention of Alizarin Red S, the stained cells were extracted with 500 μL of 10 w/v% cetylpyridinium chloride in trisodium phosphate for 15 min at room temperature, and the absorbance (OD) was measured by a microplate reader (Biorad, USA) at 570 nm.

2.4. Statistical Analysis. Experimental data were expressed as mean ± standard deviation (S.D.). The significance of differences in means was determined using least significant difference (LSD) method.

3. RESULTS

3.1. Surface Chemistry. The surface chemistry of the plasma-polymerized coatings employed in this study was characterized by XPS. The survey spectra of the coatings and the corresponding carbon to oxygen (C/O) ratios are shown in Figure 1a. The peaks at 284.8 and 531.0 eV were present in all samples and assigned to C 1s and O 1s, respectively. The peak at 398.0 eV, corresponding to N 1s, was detected in ppAAm only. The C/O ratio was lowest for ppAAc at 2.026 and highest for ppAAm at 7.002. These distinguished differences indicate the different chemical compositions in the different samples. In addition, the high-resolution C 1s spectra are shown in Figure 1b. The C 1s spectrum of ppAAc can accommodate at least four components: the peak centered at 284.8 eV is characteristic of the internal units of the C−H or/and C−C aliphatic bonds; the peaks at 286.3 and 287.9 eV can be assigned to the C−O bond and C═O bond, respectively; and the peak at 289.0 eV corresponds to the carbolyl acid group (COOH).[26] The ppAAm C 1s peak can be fitted with three components: one at 284.8 eV, another at 286.3 eV accounting for the C−N bond, and a third component at 287.6 eV which can be assigned to C═N bond. These type of films are also known to carry a significant population of amine groups, which are difficult to extract from the XPS spectra.[27] The C 1s peak of ppET can accommodate three components: one at 284.8 eV, one at 286.3 eV, and one at 287.9 eV, which can be assigned to the C−H or/and C−C, C−O, and C═O bond, respectively.[28,29] It should be noted that oxygen was also detected in the ppOD (shown in Figure 1a), although there is no oxygen in OD structure. In C 1s of ppOD, except for the peak at 284.8 eV, which corresponds to the aliphatic carbon, two other peaks were also detected: at 286.3 eV (C−O) and 287.9 eV (C═O). The results are consistent with published studies of plasma-polymerized films deposited from AAc, AAm, ET, and OD, which indicate that their coatings contain a significant

dx.doi.org/10.1021/am502170s | ACS Appl. Mater. Interfaces 2014, 6, 9733−9741

population of carboxyl (−COOH), amine ($-NH_2$), hydroxyl (−OH), and methyl ($-CH_3$) functional groups, respectively.[24,25,29−31]

3.2. Water Contact Angle. The wettability was determined by measuring the water contact angle (WCA) on plasma-polymerized coatings employed in this study. The results are shown in Figure 2, together with the representative images of

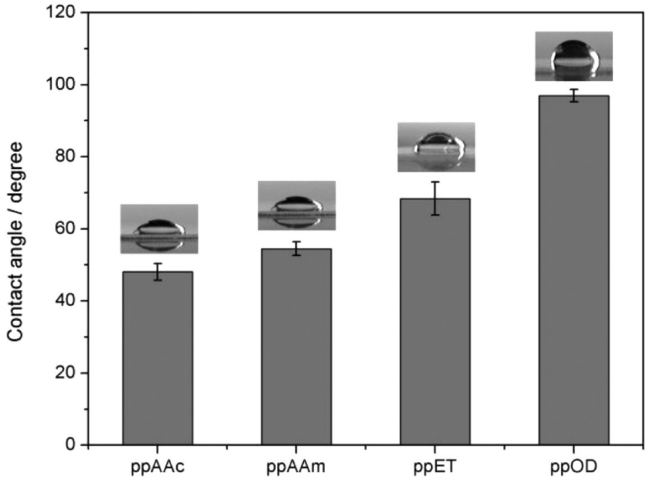

Figure 2. Water contact angles (WCAs) of different samples. Data were expressed as means ± SD (n = 4 for each sample). The representative images of water drops on different samples are also shown above each column.

the corresponding water droplets. It can be seen that there are obvious differences in the wetting properties of the coatings. The ppOD is the most hydrophobic surface with a WCA of 96.9° ± 1.7°, while ppAAc is the most hydrophilic, with a WCA of 48.1° ± 2.3°. The WCAs on ppAAm and ppET samples are 54.5° ± 1.9° and 68.4° ± 4.6°, respectively. These results confirm that changes in surface chemical compositions can affect the wettability of the materials, which is a useful parameter that has often been strongly correlated with the cell-biomaterial interfacial interactions.[32]

3.3. Atomic Force Microscopy. Surface topography has been demonstrated to affect cellular behavior. That is why the surfaces of the plasma-polymerized films were characterized by AFM. Figure 3 shows the representative images of the surface topography of the four coatings used in this study. As can be seen, all the thin plasma-polymerized films are uniform and pinhole-free. No significant features were observed in the topography of four samples. The root-mean-square (RMS) roughness was in the range of 0.2−0.3 nm, indicating a smooth surface for all samples.

Together, the surface chemical, topographical, and wettability analysis of the samples confirm that we were able to achieve four substantially different plasma-polymerized coatings in terms of chemistry and wettability, but all very smooth and homogeneous.

3.4. Cell Morphology. Anchorage-dependent cells (hASCs included) need to adhere in order to proliferate and function normally.[32] Figure 4 shows the F-actin staining images of hASCs adhered to different samples after 24 h of culture. The formation of F-actin cytoskeleton network is important to cell behavior, including cell attachment, cell shape, cell migration, etc. As it can be seen, hASCs cultured on ppAAm, ppAAc, and ppET samples all demonstrated a well-defined cytoskeleton and spread well with a polygonal morphology. The actin filaments can be observed in hASCs cultured on ppAAm, ppAAc, and ppET samples. In contrast, hASCs cultured on the ppOD sample, which is relatively hydrophobic, appeared relatively round in morphology. Sparse actin filaments were observed in hASCs cultured on ppOD samples, indicating a deficiency in cytoskeleton formation.

3.5. Cell Proliferation. To evaluate the effect of surface chemical compositions on hASCs proliferation, the CCK-8 tests were carried out to determine the viable cells number on different substrates cultured in GM with (+) and without (−) OS on day 2 and day 8 after seeding. As shown in Figure 5, similar trends are found in different samples with or without OS. hASCs numbers increased from day 2 to day 8 on all samples with or without OS. Statistically, there are no significant differences among ppAAm, ppAAc, and ppET samples, regardless, at day 8, with or without OS ($p > 0.05$). In contrast, the number of viable cells on ppOD samples is significant less than that on other three samples ($p < 0.01$), indicating that the ppOD surface, which is rich in $-CH_3$ group and relatively hydrophobic, has an inhibitory effect on the proliferation of hASCs.

3.6. Cell Osteogenic Differentiation. Alkaline phosphatase (ALP) activity assay and Alizarin Red S staining for accumulated calcium were employed to evaluate the effect of plasma-polymerized coatings on the osteogenic differentiation of hACSs. The ALP activity of hASCs cultured in growth medium with (+) or without (−) OS for 10 days is shown in Figure 6. The ALP activity is performed as a unit of King Unit per μg protein. ALP is expressed very early during the osteogenic differentiation process and is continuously associated with the region of highest ossification.[33] As expected, the ALP activity is higher in the medium with OS than without OS. Among all the groups, regardless of whether the medium was with or without OS, the ALP activity of hACSs on ppAAm is significantly higher than that on other three coatings.

After cultured with OS for 14 days, the cell layers on different samples were stained with Alizarin Red S to visualize the mineralized nodules. The staining is ascribed to predominant binding of the Alizarin Red S molecule to Ca^{2+} by forming an orange-red precipitate, easily distinguished from the background.[34,35] As shown in Figure 7a, more deposition sites of calcium are found on ppAAm. The quantitative result of retention of Alizarin Red S (Figure 7b) also reveals a significant difference between the ppAAm and the other three coatings ($p < 0.05$), which is accordant to the results of ALP activity.

4. DISCUSSION

Here, we reported the plasma polymerization method for the surface modification to enhance the osteogenic differentiation of hASCs. Allylamine (AAm), acrylic acid (AAc), 1,7-octadiene (OD), and ethanol (ET) were used as precursors to fabricate surfaces with different chemical compositions. Materials used as scaffolds should be easy to sterilize. In a clinical scenario, ^{60}Co irradiation is one of the frequently used methods for sterilization. Thus, all chemical analysis was carried out after ^{60}Co irradiation. The XPS results (Figure 1) confirm that ppAAm, ppAAc, ppOD, and ppET coatings are rich in amine ($-NH_2$), carboxyl (−COOH), methyl ($-CH_3$), and hydroxyl (−OH) chemical groups, respectively, as expected. Furthermore, plasma polymerization can be employed to generate very smooth, pinhole-free, and homogeneous coatings, as shown in AFM images (Figure 3), In general, plasma-polymerized

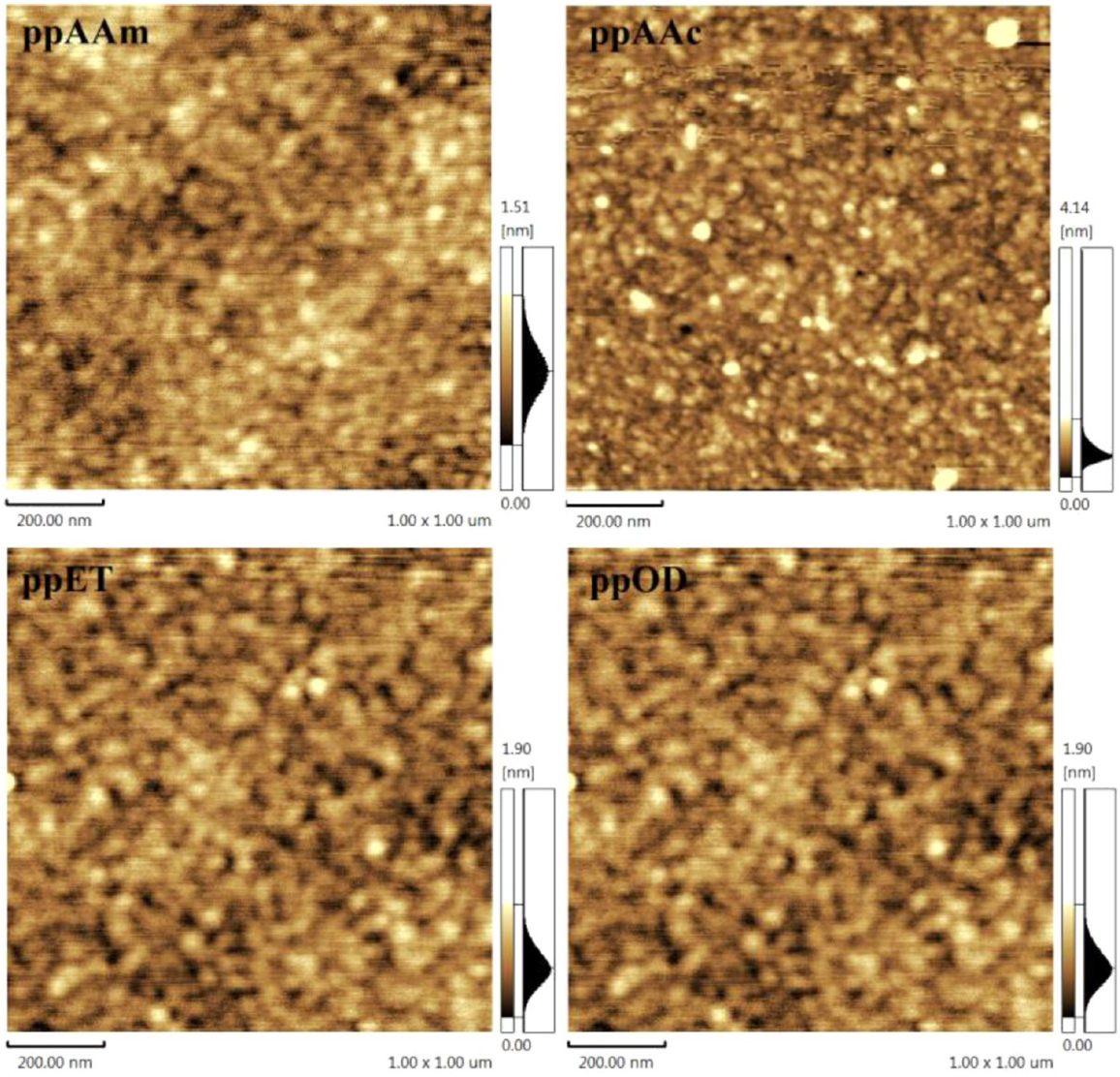

Figure 3. Representative AFM images of ppAAm, ppAAc, ppET, and ppOD. Scan size = 1 μm × 1 μm. Z-range is shown on the right side of each image. RMS of ppAAm, 0.231 nm; ppAAc, 0.307 nm; ppET, 0.270 nm; and ppOD, 0.353 nm.

coatings have been demonstrated to be stable in solvents, thermally stable, chemically inert, mechanically robust, and applicable to the surfaces on a variety of substrate materials,[22] which indicates that this is an appropriate method for surface modification of scaffolds used in bone tissue engineering.

The WCA results confirm that the change in surface chemical compositions also affect the surface wettability. The wettability is determined mostly by the charge, polarizability, and polarity of the surface functional groups.[36] The high contact angle of 96.9° ± 1.7° for ppOD sample results from the hydrophobic characteristic of $-CH_3$ functional groups.[37] The surface wettability usually does not directly mediate cell response. Instead, it affects the type and/or conformation of the proteins adsorbed to the surface from serum components, which, in turn, affects cell adhesion, proliferation, and differentiation.[38] Hydrophobic surfaces irreversibly adsorb large quantities of albumin, an abundant serum protein that does not support cell attachment.[36] That is the reason why hASCs on the ppOD sample (Figure 5) did not attach and spread well. This result is consistent with the findings of others reporting that the hydrophobic $-CH_3$-terminated SAMs do not support the attachment of fibroblasts,[39] osteoblasts[40] and hMSCs.[41] For anchorage-dependent cells, the cell proliferation is related closely to the adherence. The lowest cell number was found on the ppOD samples, indicating that the ppOD sample has an inhibitory effect on cell proliferation. By contrast, the hydrophilic surfaces (ppAAm, ppAAc, and ppET samples in this study) tend to adsorb proteins, which can promote cells adhesion,[36] such as fibronectin[40] and/or vitronectin.[39,42] They are both components of extracellular matrix (ECM) and play major roles in cell attachment. This explains why ppAAm, ppAAc, and ppET samples promote the attachment, spreading, and, in turn, proliferation of hASCs.

Although there are no significant differences in hASCs proliferation among ppAAm, ppAAc, and ppET samples, the levels of osteogenic differentiation of hASCs cultured on different samples are distinct. The ALP activity (Figure 6) and mineralization level determined by ARS staining (Figure 7) both demonstrate that the amine-rich ppAAm samples enhanced the osteogenic differentiation of hASCs. Keselowsky et al. also reported that the $-NH_2$-terminated surfaces generated by SAMs up-regulated osteoblast-specific gene

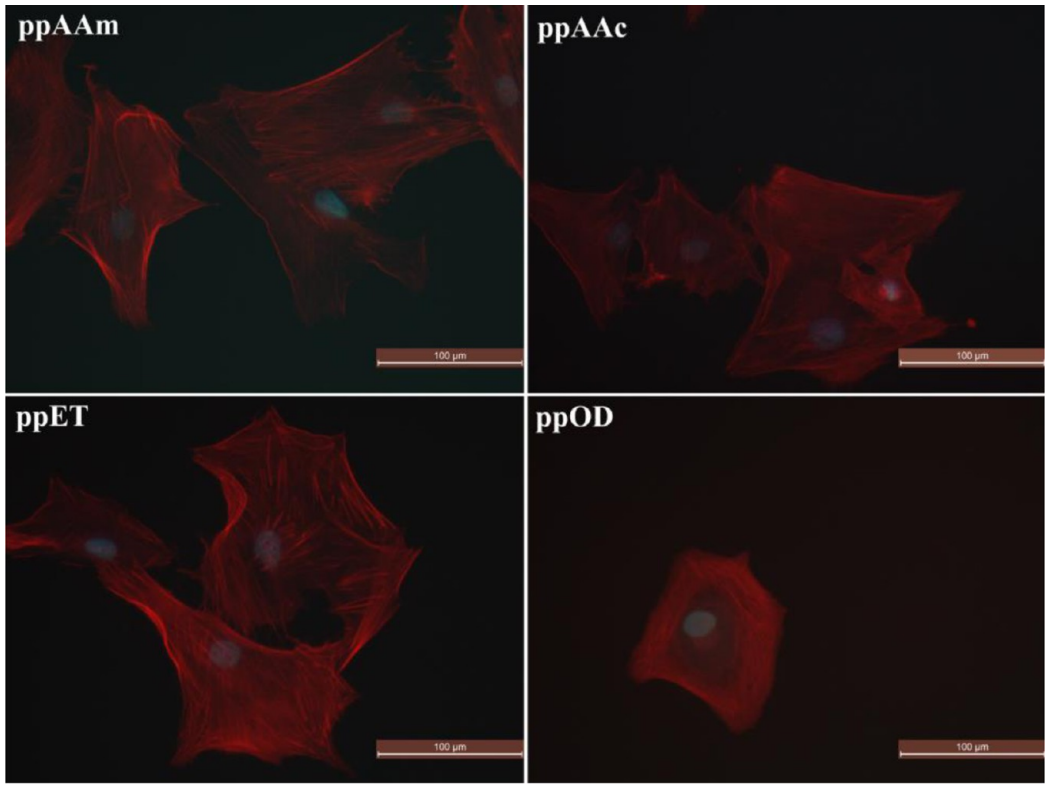

Figure 4. Fluorescence images of hASCs cultured on different samples for morphology. hASCs were cultured in medium without OS for 24 h. Cells were stained with phalloidin-TRITC for actin (red) and DAPI for cell nuclei (blue). Images were photographed under a fluorescence microscope. Scale bar = 100 μm.

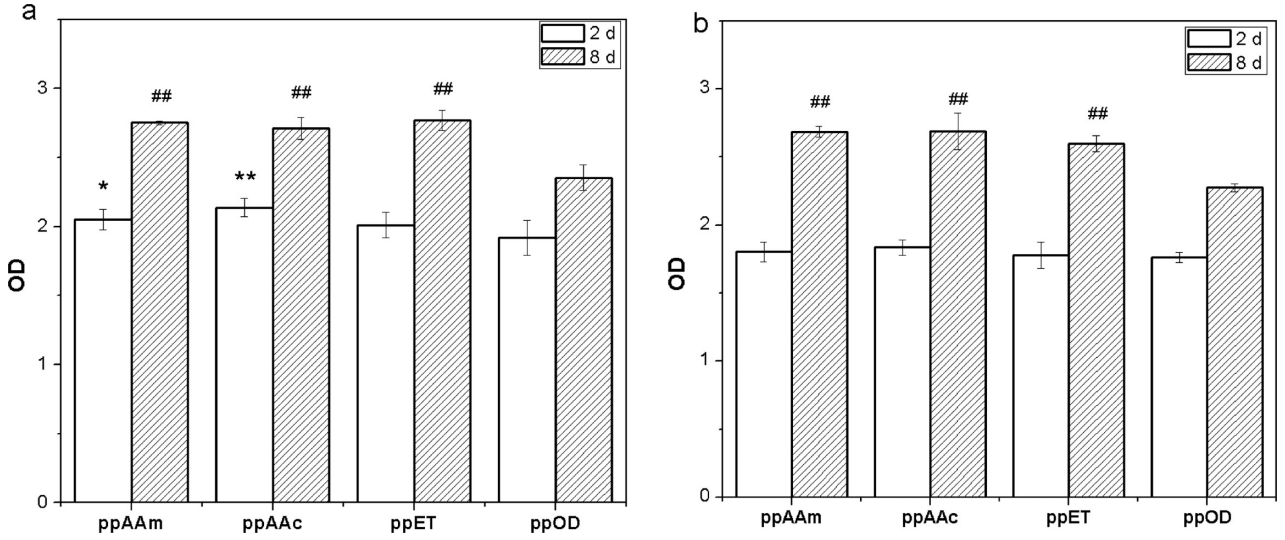

Figure 5. CCK-8 assay of hASCs cultured on different samples for proliferation in a medium (a) without OS and (b) with OS at day 2 and day 8. Data were expressed as means ± standard deviation (SD) (n = 6 for each sample). Single asterisk (*) and double asterisks (**) denote a statistical significance of $p < 0.05$ and $p < 0.01$, respectively, compared to data obtained on ppOD sample at day 2. Double pound sign (##) denotes a statistical significance of $p < 0.01$, compared to data obtained on ppOD sample at day 8.

expression, ALP activity and matrix mineralization of MC3T3-E1 cells,[12] consistent with the effects observed on osteogenesis of hMSCs (also favored by $-NH_2$ surface generated by silane modification).[13,43] Several possible mechanisms were proposed to explain how surface chemistry regulates the osteogenic differentiation. One involved is related to the surface-dependent differences in integrin binding. Integrins are a family of heterodimeric transmembrane glycoproteins consisting of α- and a β-subunits.[44] Integrin-mediated adhesion of cells to extracellular matrix components is essential for cell behaviors. Lineage-specific intergrins mediate signal transduction regulating the expression of genes controlling differentiation to a particular lineage.[45] Changes in surface chemistry can affect the conformation of fibronectin and, in turn, affect the type of binding intergrins.[38] For example, in the case of MC3T3-E1 cells, the conformational changes of fibronectin on $-NH_2$-

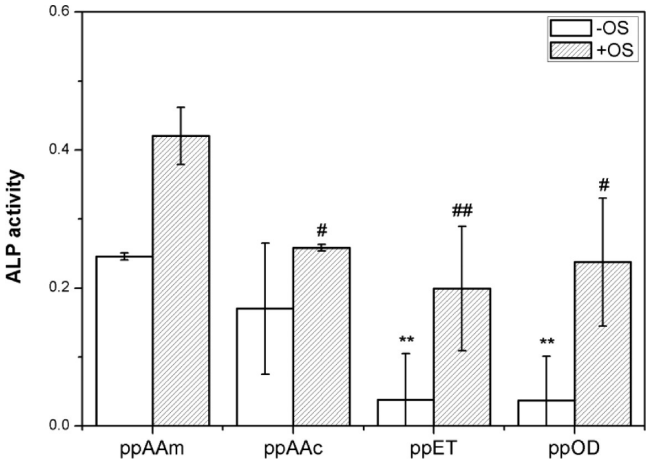

Figure 6. Normalized alkaline phosphatase activity expression by hASCs cultured on different samples in medium without (−) OS and with (+) OS at day 10. Data were expressed as means ± standard deviation (SD) (n = 4 for each sample) Double asterisks (**) denote a statistical significance of $p < 0.01$, compared to data obtained on ppAAm sample without (−) OS. Single pound sign (#) and double pound sign (##) denote a statistical significance of $p < 0.05$ and $p < 0.01$, respectively, compared to data obtained on ppAAm sample with (+) OS.

terminated surfaces generated by SAMs-promoted binding of intergrin $\alpha5\beta1$,[46] which is shown to be required for osteoblast differentiation.[47] Another possible mechanism to explain why the functionalized surfaces with $-NH_2$ enhanced the osteogenic differentiation can be attributed the positively charged property of amine groups. It has been reported that the interfacial pH on the surface of implant materials affects the osteoblast activity.[48] Both the proliferation and ALP activity of osteoblasts was significantly enhanced at a high pH value.[49] The positively charged amine groups on the surface of AAm sample provide a microenvironment of relatively high pH value, which may promote the osteogenic differentiation of hASCs.

The results shown in this work demonstrate the allylamine plasma-polymerized surface can promote osteogenic differentiation of hASCs, indicating that this is an appealing method for surface modification of scaffolds used in bone tissue engineering. To fully explore the obviously different effects of the ppAAm and ppOD on the attachment, proliferation, and osteogenic differentiation of hASCs, we are now conducting experiments with surfaces designed in a chemical functionality concentration gradient manner (from ppOD to ppAAm). hASCs were cultured on such substrates with and without fetal bovine serum (FBS) to confirm the influence of the serum proteins. As shown in the Supporting Information (Figure S1), hASCs showed a different behavior on different regions of such substrate when cultured with FBS: the cell number and spreading area increased with the gradient from ppOD to ppAAm. In contrast, the differences are not found when cultured without FBS. FBS is rich in different proteins such as albumin, fibronectin, vitronectin, etc. It may be an evidence to support that the surface chemistries affect the behavior of hASCs by the interaction with the serum proteins. However, further research is required to confirm the conformational changes of absorbed proteins and the type of binding intergrins, and/or how the interfacial pH affects the osteogenic differentiation of hASCs.

5. CONCLUSION

In this study, allylamine (AAm), acrylic acid (AAc), 1,7-octadiene (OD), and ethanol (ET) were used as precursors for plasma polymerization in order to generate thin films rich in amine ($-NH_2$), carboxyl ($-COOH$), methyl ($-CH_3$), and hydroxyl ($-OH$) functional groups, respectively. The results demonstrate that the surface chemical compositions generated by plasma polymerization can affect behavior, especially the osteogenic differentiation of hASCs. Among all samples, ppAAm sample can promote the attachment, spreading, and, in turn, proliferation of hASCs, as well as promote the osteogenic differentiation of hASCs. The results demonstrate that plasma polymerization is an appealing method for the surface modification of scaffolds used in bone tissue engineering. Further research in our lab is directed to deriving a mechanistic explanation of the findings reported in this paper.

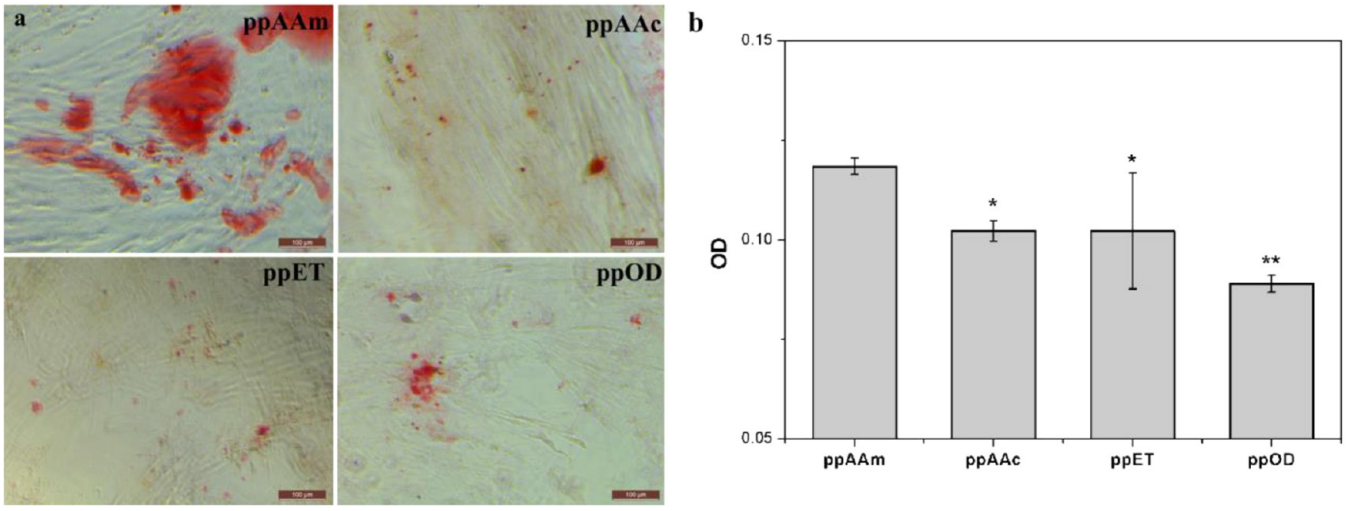

Figure 7. (a) Alizarin Red S staining for mineral deposition formed by hASCs cultured on different samples in medium with OS at day 14. (b) The quantitative result of retention of Alizarin Red. Data were expressed as means ± SD (n = 4 for each sample). Single asterisk (*) and double asterisks (**) denote a statistical significance of $p < 0.05$ and $p < 0.01$, respectively, compared to data obtained on the ppAAm sample.

■ ASSOCIATED CONTENT

Supporting Information

Additional figure shows the Calcein-AM staining of hASCs cultured on substrate with surface gradients (from ppOD to ppAAm) for 24 h with and without FBS. This material is available free of charge via the Internet at http://pubs.acs.org.

■ AUTHOR INFORMATION

Corresponding Author

*E-mail: biomater@mail.tsinghua.edu.cn.

Notes

The authors declare no competing financial interest.

■ ACKNOWLEDGMENTS

The authors are grateful for the financial support from National Natural Science Foundation of China (No. 51361130032) and Doctor Subject Foundation of the Ministry of Education of China (No. 20120002130002). K.V. thanks ARC for a fellowship (No. FT100100292).

■ REFERENCES

(1) Hutmacher, D. W. Scaffolds in Tissue Engineering Bone and Cartilage. *Biomaterials* **2000**, *21*, 2529−2543.
(2) Nerem, R. M. Tissue Engineering: the Hope, the Hype, and the Future. *Tissue Eng.* **2006**, *12*, 1143−1150.
(3) Chan, B. P.; Leong, K. W. Scaffolding in Tissue Engineering: General Approaches and Tissue-Specific Considerations. *Eur. Spine J.* **2008**, *17* (Suppl. 4), 467−79.
(4) Yang, K.; Jung, K.; Ko, E.; Kim, J.; Park, K. I.; Kim, J.; Cho, S. Nanotopographical Manipulation of Focal Adhesion Formation for Enhanced Differentiation of Human Neural Stem Cells. *ACS Appl. Mater. Interfaces* **2013**, *5*, 10529−10540.
(5) Brunner, E. W.; Jurewicz, I.; Heister, E.; Fahimi, A.; Bo, C.; Sear, R. P.; Donovan, P. J.; Dalton, A. B. Growth and Proliferation of Human Embryonic Stem Cells on Fully Synthetic Scaffolds Based on Carbon Nanotubes. *ACS Appl. Mater. Interfaces* **2014**, *6*, 2598−2603.
(6) Shabani, I.; Haddadi-Asl, V.; Soleimani, M.; Seyedjafari, E.; Hashemi, S. M. Ion-exchange Polymer Nanofibers for Enhanced Osteogenic Differentiation of Stem Cells and Ectopic Bone Formation. *ACS Appl. Mater. Interfaces* **2013**, *6*, 72−82.
(7) Nam, J.; Johnson, J.; Lannutti, J. J.; Agarwal, S. Modulation of Embryonic Mesenchymal Progenitor Cell Differentiation via Control over Pure Mechanical Modulus in Electrospun Nanofibers. *Acta Biomater.* **2011**, *7*, 1516−1524.
(8) Brammer, K. S.; Choi, C.; Frandsen, C. J.; Oh, S.; Jin, S. Hydrophobic Nanopillars Initiate Mesenchymal Stem Cell Aggregation and Osteo-Differentiation. *Acta Biomater.* **2011**, *7*, 683−690.
(9) Weinand, C.; Pomerantseva, I.; Neville, C. M.; Gupta, R.; Weinberg, E.; Madisch, I.; Shapiro, F.; Abukawa, H.; Troulis, M. J.; Vacanti, J. P. Hydrogel-β-TCP Scaffolds and Stem Cells for Tissue Engineering Bone. *Bone (N.Y., N.Y., U.S.)* **2006**, *38*, 555−563.
(10) Baer, P. C.; Griesche, N.; Luttmann, W.; Schubert, R.; Luttmann, A.; Geiger, H. Human Adipose-Derived Mesenchymal Stem Cells *in vitro*: Evaluation of an Optimal Expansion Medium Preserving Stemness. *Cytotherapy* **2010**, *12*, 96−106.
(11) Zanetti, A. S.; Sabliov, C.; Gimble, J. M.; Hayes, D. J. Human Adipose-Derived Stem Cells and Three-Dimensional Scaffold Constructs: A Review of the Biomaterials and Models Currently Used for Bone Regeneration. *J. Biomed. Mater. Res., Part B* **2013**, *101B*, 187−199.
(12) Keselowsky, B. G.; Collard, D. M.; Garcia, A. J. Integrin Binding Specificity Regulates Biomaterial Surface Chemistry Effects on Cell Differentiation. *Proc. Natl. Acad. Sci. U. S. A.* **2005**, *102*, 5953−5957.
(13) Curran, J. M.; Chen, R.; Hunt, J. A. Controlling The Phenotype and Function of Mesenchymal Stem Cells *in vitro* By Adhesion to Silane-Modified Clean Glass Surfaces. *Biomaterials* **2005**, *26*, 7057−7067.
(14) Keselowsky, B. G.; Collard, D. M.; Garcia, A. J. Surface Chemistry Modulates Focal Adhesion Composition and Signaling Through Changes in Integrin Binding. *Biomaterials* **2004**, *25*, 5947−5954.
(15) Collart-Dutilleul, P.; Secret, E.; Panayotov, I.; Deville De Périère, D.; Martín-Palma, R. J.; Torres-Costa, V.; Martin, M.; Gergely, C.; Durand, J.; Cunin, F.; Cuisinier, F. J. Adhesion and Proliferation Of Human Mesenchymal Stem Cells from Dental Pulp on Porous Silicon Scaffolds. *ACS Appl. Mater. Interfaces* **2014**, *6*, 1719−1728.
(16) Kuddannaya, S.; Chuah, Y. J.; Lee, M. H. A.; Menon, N. V.; Kang, Y.; Zhang, Y. Surface Chemical Modification of Poly-(Dimethylsiloxane) for the Enhanced Adhesion and Proliferation of Mesenchymal Stem Cells. *ACS Appl. Mater. Interfaces* **2013**, *5*, 9777−9784.
(17) Chieh, H.; Su, F.; Lin, S.; Shen, M.; Liao, J. Migration Patterns and Cell Functions of Adipose-Derived Stromal Cells on Self-Assembled Monolayers with Different Functional Groups. *J. Biomater. Sci., Polym. Ed.* **2012**, 1−24.
(18) Bai, B.; He, J.; Li, Y.; Wang, X.; Ai, H.; Cui, F. Activation of the ERK1/2 Signaling Pathway During the Osteogenic Differentiation of Mesenchymal Stem Cells Cultured on Substrates Modified with Various Chemical Groups. *BioMed. Res. Int.* **2013**, *2013*, 15.
(19) Liu, X.; He, J.; Zhang, S.; Wang, X.; Liu, H.; Cui, F. Adipose Stem Cells Controlled by Surface Chemistry. *J. Tissue Eng. Regener. Med.* **2013**, *7*, 112−117.
(20) Senaratne, W.; Andruzzi, L.; Ober, C. K. Self-assembled Monolayers and Polymer Brushes in Biotechnology: Current Applications and Future Perspectives. *Biomacromolecules* **2005**, *6*, 2427−2448.
(21) Low, S. P.; Short, R. D.; Steele, D. A. Plasma Polymer Surfaces for Cell Expansion and Delivery. *J. Adhes. Sci. Technol.* **2010**, *24*, 2215−2236.
(22) Jacobs, T.; Morent, R.; De Geyter, N.; Dubruel, P.; Leys, C. Plasma Surface Modification of Biomedical Polymers: Influence on Cell-Material Interaction. *Plasma Chem. Plasma Process.* **2012**, *32*, 1039−1073.
(23) Vasilev, K. Nanoengineered Plasma Polymer Films for Biomaterial Applications. *Plasma Chem. Plasma Process.* **2013**, *34*, 1−14.
(24) Vasilev, K.; Michelmore, A.; Martinek, P.; Chan, J.; Sah, V.; Griesser, H. J.; Short, R. D. Early Stages of Growth of Plasma Polymer Coatings Deposited from Nitrogen- and Oxygen-Containing Monomers. *Plasma Processes Polym.* **2010**, *7*, 824−835.
(25) Vasilev, K.; Michelmore, A.; Griesser, H. J.; Short, R. D. Substrate Influence on The Initial Growth Phase of Plasma-Deposited Polymer Films. *Chem. Commun. (Cambridge, U.K.)* **2009**, 3600−3602.
(26) Detomaso, L.; Gristina, R.; Senesi, G. S.; D Agostino, R.; Favia, P. Stable Plasma-Deposited Acrylic Acid Surfaces for Cell Culture Applications. *Biomaterials* **2005**, *26*, 3831−3841.
(27) Mierczynska, A.; Michelmore, A.; Tripathi, A.; Goreham, R. V.; Sedev, R.; Vasilev, K. pH-Tunable Gradients of Wettability and Surface Potential. *Soft Matter* **2012**, *8*, 8399−8404.
(28) Xu, Z.; Yang, L.; Fan, X.; Jin, J.; Mei, J.; Peng, W.; Jiang, F.; Xiao, Q.; Liu, Y. Low Temperature Synthesis of Highly Stable Phosphate Functionalized Two Color Carbon Nanodots and Their Application in Cell Imaging. *Carbon* **2014**, *66*, 351−360.
(29) Hazrati, H. D.; Whittle, J. D.; Vasilev, K. A Mechanistic Study of the Plasma Polymerization of Ethanol. *Plasma Processes Polym.* **2014**, *11*, 149−157.
(30) Akhavan, B.; Jarvis, K.; Majewski, P. Evolution of Hydrophobicity in Plasma Polymerised 1,7-Octadiene Films. *Plasma Processes Polym.* **2013**, *10*, 1018−1029.
(31) Michelmore, A.; Martinek, P.; Sah, V.; Short, R. D.; Vasilev, K. Surface Morphology in the Early Stages of Plasma Polymer Film Growth from Amine-Containing Monomers. *Plasma Processes Polym.* **2011**, *8*, 367−372.

(32) Lopez-Perez, P. M.; Marques, A. P.; Silva, R. M. P. D.; Pashkuleva, I.; Reis, R. L. Effect of Chitosan Membrane Surface Modification via Plasma Induced Polymerization on the Adhesion of Osteoblast-Like Cells. *J. Mater. Chem.* **2007**, *17*, 4064−4071.
(33) Müller, W. E.; Wang, X.; Grebenjuk, V.; Diehl-Seifert, B.; Steffen, R.; Schloßmacher, U.; Trautwein, A.; Neumann, S.; Schröder, H. C. Silica as a Morphogenetically Active Inorganic Polymer. *Biomater. Sci.* **2013**, *1*, 669−678.
(34) Moriguchi, T.; Yano, K.; Nakagawa, S.; Kaji, F. Elucidation of Adsorption Mechanism of Bone-Staining Agent Alizarin Red S on Hydroxyapatite by FT-IR Microspectroscopy. *J. Colloid Interface Sci.* **2003**, *260*, 19−25.
(35) Paul, H.; Reginato, A. J.; Ralph Schumacher, H. Alizarin Red S Staining as a Screening Test to Detect Calcium Compounds in Synovial Fluid. *Arthritis Rheum.* **1983**, *26*, 191−200.
(36) Mager, M. D.; LaPointe, V.; Stevens, M. M. Exploring and Exploiting Chemistry at the Cell Surface. *Nat. Chem.* **2011**, *3*, 582−9.
(37) Mendoza, S. M.; Arfaoui, I.; Zanarini, S.; Paolucci, F.; Rudolf, P. Improvements in the Characterization of the Crystalline Structure of Acid-Terminated Alkanethiol Self-Assembled Monolayers on Au (111). *Langmuir* **2006**, *23*, 582−588.
(38) Phadke, A.; Chang, C.; Varghese, S. In *Biomaterials as Stem Cell Niche*; Krishnendu, R., Ed.; Springer: Berlin, 2010; Chapter 2, pp 19−44.
(39) Faucheux, N.; Schweiss, R.; Lützow, K.; Werner, C.; Groth, T. Self-Assembled Monolayers with Different Terminating Groups as Model Substrates for Cell Adhesion Studies. *Biomaterials* **2004**, *25*, 2721−2730.
(40) Scotchford, C. A.; Gilmore, C. P.; Cooper, E.; Leggett, G. J.; Downes, S. Protein Adsorption and Human Osteoblast-Like Cell Attachment and Growth on Alkylthiol on Gold Self-Assembled Monolayers. *J. Biomed. Mater. Res.* **2002**, *59*, 84−99.
(41) Phillips, J. E.; Petrie, T. A.; Creighton, F. P.; García, A. J. Human Mesenchymal Stem Cell Differentiation on Self-Assembled Monolayers Presenting Different Surface Chemistries. *Acta Biomater.* **2010**, *6*, 12−20.
(42) Chieh, H.; Su, F.; Liao, J.; Lin, S.; Chang, C.; Shen, M. Attachment and Morphology of Adipose-Derived Stromal Cells and Exposure of Cell-Binding Domains of Adsorbed Proteins on Various Self-Assembled Monolayers. *Soft Matter* **2011**, *7*, 3808−3817.
(43) Curran, J. M.; Chen, R.; Hunt, J. A. The Guidance of Human Mesenchymal Stem Cell Differentiation *in vitro* by Controlled Modifications to the Cell Substrate. *Biomaterials* **2006**, *27*, 4783−4793.
(44) Legler, D. F.; Wiedle, G.; Ross, F. P.; Imhof, B. A. Superactivation of Integrin (α)v(β)3 by Low Antagonist Concentrations. *J. Cell Sci.* **2001**, *114*, 1545−1553.
(45) Yamada, K. M.; Miyamoto, S. Integrin Transmembrane Signaling and Cytoskeletal Control. *Curr. Opin. Cell Biol.* **1995**, *7*, 681−689.
(46) Keselowsky, B. G.; Collard, D. M.; Garcia, A. J. Surface Chemistry Modulates Fibronectin Conformation and Directs Integrin Binding and Specificity to Control Cell Adhesion. *J. Biomed. Mater. Res., Part A* **2003**, *66A*, 247−259.
(47) Moursi, A. M.; Globus, R. K.; Damsky, C. H. Interactions Between Integrin Receptors and Fibronectin Are Required for Calvarial Osteoblast Differentiation *in vitro*. *J. Cell Sci.* **1997**, *110*, 2187−2196.
(48) Shen, Y.; Liu, W.; Wen, C.; Pan, H.; Wang, T.; Darvell, B. W.; Lu, W. W.; Huang, W. Bone Regeneration: Importance of Local pH-Strontium-Doped Borosilicate Scaffold. *J. Mater. Chem.* **2012**, *22*, 8662−8670.
(49) Shen, Y.; Liu, W.; Lin, K.; Pan, H.; Darvell, B. W.; Peng, S.; Wen, C.; Deng, L.; Lu, W. W.; Chang, J. Interfacial pH: A Critical Factor for Osteoporotic Bone Regeneration. *Langmuir* **2011**, *27*, 2701−2708.